The final publication is available at

http://dx.doi.org/10.1109/TIE.2012.2222855

Efficiency and Fault-Ride-Through Performance of a Diode-Rectifier and VSC-Inverter based HVDC Link for Off-shore Wind Farms

S. Bernal-Perez, S. Añó-Villalba, R. Blasco-Gimenez, *Senior Member, IEEE*, J. Rodríguez-D'Derlée, *Student Member, IEEE*

Abstract—This paper includes a technical feasibility study on the use of a HVDC diode based rectifier together with an on-shore voltage source converter for the connection of large off-shore wind farms. A distributed control algorithm for the wind farm is used, where all the wind turbines contribute to the off-shore grid voltage and frequency control, while allowing wind turbine optimal power tracking. Moreover, the proposed system shows good fault ride-through performance to solid faults at on-shore connection point, wind farm ac-grid and HVDC line. The technical feasibility of the proposed solution has been validated by means of detailed PSCAD simulations. The efficiency of the complete system has also been studied and found to compare favorably with that of a VSC-HVDC rectifier station.

Index Terms—HVDC transmission control, Wind power generation, Current control, Voltage control, Frequency control, Power generation control.

I. INTRODUCTION

DIODE based rectifiers for unidirectional HVDC links have been suggested in the past as an alternative to increase efficiency and system reliability [1]–[3]. The lack of flexible control and the convenience of keeping bidirectional power flow capability have been important deterrents to the use of HVDC diode based rectifiers. However, the integral design of the wind turbine, off-shore ac-grid and HVDC link has shown that a diode based HVDC rectifier can be used for the connection of a large wind farm with steady state and transient performance similar to that of traditional line commutated thyristor (LCT) HVDC links [4], [5].

On the other hand, the use of Voltage Source Converter (VSC) HVDC links offers distinctive advantages, arising from the faster and more flexible active and reactive power control and from shorter design and installation times [6], [7].

Alternative proposals for the HVDC connection of large off-shore wind farms also include the series connection of
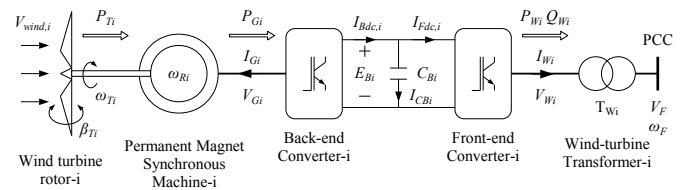
Fig. 1. Off-shore aggregated wind turbine i (i=1,2,..,5) connected to the off-shore PCC

the different wind turbines [8], [9]. However, these alternative topologies lead to load dependent HVDC voltage [8] and to stringent isolation requirements of generators [8] or wind turbine transformers [9], which are still object of ongoing research.

The use of an off-shore HVDC diode rectifier together with an on-shore VSC inverter for the connection of off-shore wind farms was initially proposed in [10], albeit connected to a relatively strong transmission network. Important aspects, such as connection to weak transmission networks, overall system efficiency and ride-through performance to different faults still remain to be addressed.

An important advantage of of LCC-HVDC links over their VSC counterparts is the lower equipment cost and use of higher voltages, which leads to reduced transmission losses [11], [12]. However, the voltage advantage is lost when a hybrid link like the one proposed in this paper is used.

Moreover, the capacitor and filter banks of LCC-HVDC converters are much larger than the filtering required for VSC-HVDC stations, representing additional losses and expenses.

Therefore, a comparison of the relative efficiency of the proposed topology with respect to a VSC-HVDC rectifier will be carried out.

This paper also includes the validation of wind turbine and VSC inverter fault ride through strategies against short circuits at the onshore PCC, off-shore ac-grid and HVDC line.

There is an increasing trend on different manufacturers on the use of fully rated converters for wind turbines for off-shore applications [13], [14], and there is active research on the development of new, more robust converter topologies [15]. Therefore, the proposed control strategies assume wind turbines with fully rated converters.

Fig. 2. HVDC link (uncontrolled rectifier and VSC inverter) and on-shore ac-grid

Fig. 3. VSC dc-voltage (E_I) control loop

II. SYSTEM MODELLING AND CONTROL

The system under study is shown in Figs. 1 and 2. The considered wind farm has an installed power of 400 MW and is modeled using five aggregated wind turbines of different rating: 5, 40, 80, 120 and 155 MW.

Fig. 2 shows the HVDC transmission link consisting on an off-shore 12-pulse diode-based rectifier and an on-shore Voltage Source Converter (VSC). Z_{FR} represents both the rectifier shunt capacitor C_F and the harmonic filter banks.

The wind turbine generators are controlled by their respective back-end converters using standard field-oriented control. The generator torque current is used to keep the back-to-back converter dc-link voltage to its reference. Therefore, the wind turbine front-end currents can be freely set to follow any desired reference [4].

A. Off-shore ac-grid Voltage and Frequency Control

The dynamics of the off-shore ac-grid, in a synchronous-frame rotating at ω_F and oriented on V_F, can be written as

$$\frac{d}{dt}V_{Fd} = \frac{1}{C_F}\sum_{i=1}^{5} I_{Wdi} - \frac{1}{C_F}I_{FRd} \qquad (1)$$

$$\omega_F V_{Fd} = \frac{1}{C_F}\sum_{i=1}^{5} I_{Wqi} - \frac{1}{C_F}I_{FRq} \qquad (2)$$

The front-end converter currents I_{Wdi} and I_{Wqi} are controlled by means of fast current control loops based on $d-q$ frame PI controllers. The overall wind farm active current $I_{Fd} = \sum_{i=1}^{5} I_{Wdi}$ can be used to control the off-shore ac-grid voltage V_{Fd} [4].

From (2), the overall current $I_{Fq} = \sum_{i=1}^{5} I_{Wqi}$ can be used to control the off-shore ac-grid frequency ω_F with a proportional controller. The remote current I_{FRq} has been estimated using local measurements.

A more detailed analysis of the off-shore ac-grid voltage and frequency control can be found in [5].

B. On-shore VSC-Inverter Modeling and Control

The VSC active and reactive currents (I_{Vd}, I_{Vq}) are controlled on a $d-q$ synchronous frame oriented on V_S with a 40 Hz bandwidth.

Conduction and commutation losses of the VSC are neglected, therefore $P_{Vdc} = P_V$, hence
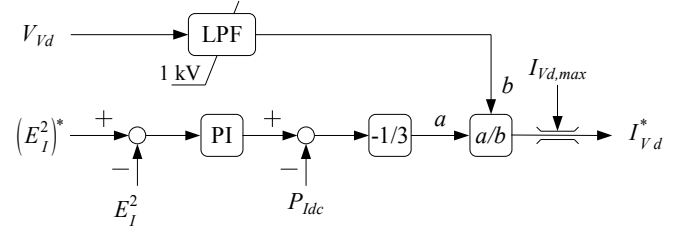
$$P_{Vdc} = E_I I_{Vdc} \qquad (3)$$
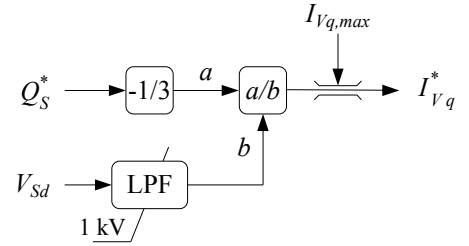
and

$$P_V = 3(V_{Vd}I_{Vd} + V_{Vq}I_{Vq}) \qquad (4)$$

Since the dynamics of E_I is

$$\frac{d}{dt}E_I = \frac{1}{C_I}I_{Idc} - \frac{1}{C_I}I_{Vdc} \qquad (5)$$

then the relationship between E_I and I_{Vd}^* can be drawn using (3) and (4)

$$\frac{dE_I^2}{dt} = \frac{2}{C_I}I_{Idc}E_I - \frac{6}{C_I}V_{Vd}I_{Vd}^* - \frac{6}{C_I}V_{Vq}I_{Vq} \qquad (6)$$

After linearization, assuming $V_{Vq} \approx 0$ and using $P_{Idc} = E_I I_{Idc}$, the result is

$$\frac{C_I}{2}\Delta\left(\frac{dE_I^2}{dt}\right) \approx \Delta P_{Idc} - 3V_{Vd0}\Delta I_{Vd}^* \qquad (7)$$

The proposed control scheme is depicted in Fig. 3. The bandwidth of the E_I^2 control loop is set to 4 Hz and a limit is imposed to the current reference I_{Vd}^* for protection purposes.

As is shown in Fig. 4, I_{Vq}^* is calculated from the reactive power demand Q_S^*, considering the current limit $I_{Vq,max}$.

III. OPTIMUM POWER TRACKING

During normal operation, the diode rectifier acts as a voltage clamp on the off-shore ac-grid voltage V_{Fd}. Therefore, E_R will be roughly proportional to the HVDC voltage V_{Fd}. The off-shore grid voltage reference V_{Fd}^* is set above the clamped voltage. Therefore, the controller will increase the wind turbine current reference (I_{Wdi}^*) until it reaches its limit. This limit is fixed either by the wind turbine optimum power characteristic (P_{Wi}^*), or by fault protection mechanisms [5].

Therefore, during normal operation, the different wind turbines will be injecting their optimal power reference (P_{Wi}^*).

Fig. 5 shows the maximum optimal power that can be extracted from the wind, together with the actual power
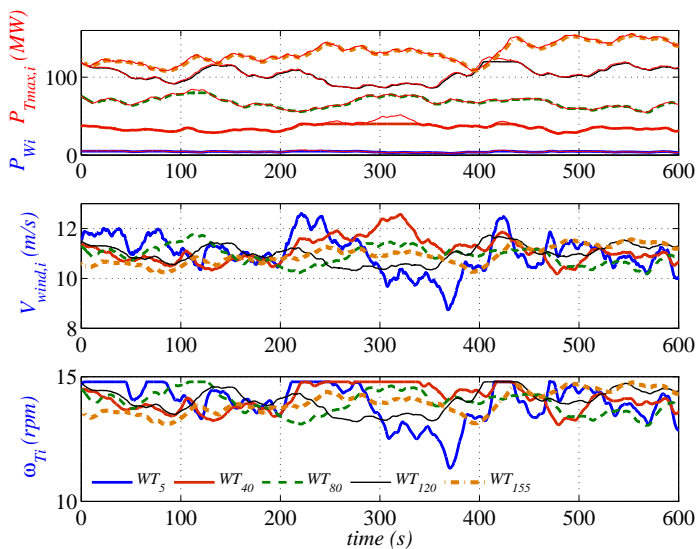
Fig. 5. Optimum power tracking of each wind turbine cluster ($v = 11$ m/s, $\sigma = 10\%$).
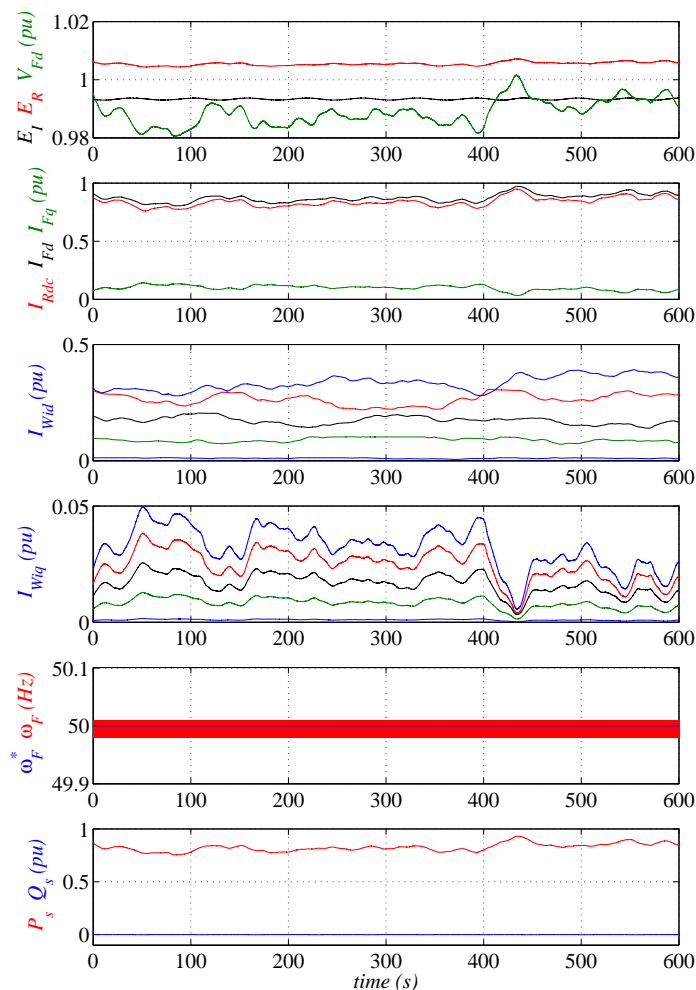

Fig. 6. Wind farm optimum power tracking ($v = 11$ m/s, $\sigma = 10\%$).

extracted by each cluster of wind turbines. The wind speed for each cluster of wind turbines has been generated assuming a ten minute average hub wind speed of 11 m/s, with a turbulence intensity of 10%, following a Kaimal distribution. The instantaneous hub wind speed has been used to calculate an averaged rotor wind speed, neglecting rotational sampling or tower shadow effects. The number of wind turbines on each cluster has been considered for the calculation of the cluster averaged wind speed, assuming that wind speeds are uncorrelated among the different wind turbines.

Although wind farm scale effects have not been taken into account, the frequency contents of the simulated wind speeds are adequate to evaluate optimum power tracking performance.

Fig. 5 shows the wind turbines closely following the optimum available wind energy. Moreover, when available wind power exceeds the wind turbine capability, pitch control keeps the wind turbine power and speed at their rated values.

Fig. 5 also shows the averaged wind speed ($V_{wind,i}$) and wind turbine speed (ω_{Ti}) for each one of the clusters.

System behaviour for aforementioned wind conditions is shown in Fig. 6. The wind farm ac voltage is kept under control between a 2% band of its rated value. The variation on HVDC sending and receiving end voltages (E_R, E_I) is much smaller.

Notice wind turbine active currents follow the individual optimal characteristic while the reactive power needed for adequate frequency control is correctly shared amongst wind turbines clusters.

The off-shore frequency ω_F shows some ripple caused by V_F harmonics. This ripple is not symmetrical, however, its average value is kept at 50 Hz at all times. The active power delivered by the on-shore VSC-HVDC station (P_s) follows the variations on the wind farm active current, while Q_s remains at its zero reference value.

IV. POWER LOSSES AND EFFICIENCY

Estimates of HVDC station losses can vary largely from one installation to another, due to operating conditions, valve construction and many other factors. Therefore, loss studies should be carried out using measurements on actual HVDC stations [16]–[18].

As this is clearly not possible in our case, the procedure stated in [16] will be used to obtain the valve losses, whereas typical losses obtained from actual LCT-HVDC stations will be used for transformer, ac filters, smoothing reactors and ancillary equipment [16], [19].

Moreover, in order to compare the efficiency of the proposed topology with that of a VSC-HVDC solution, additional wind turbine losses caused by increased harmonics and reactive power will be considered.

A. Diode valves

Conduction losses have been calculated for two different devices, 5SDD 10F6000 and 5SDD 31H6000, whose characteristics are in table I.

Diode valve conduction losses have been calculated by integrating the instantaneous power losses over a fundamental

This article has been accepted for publication in a future issue of this journal, but has not been fully edited. Content may change prior to final publication.

4

TABLE I
DEVICES USED FOR DIODE VALVE LOSS CALCULATION

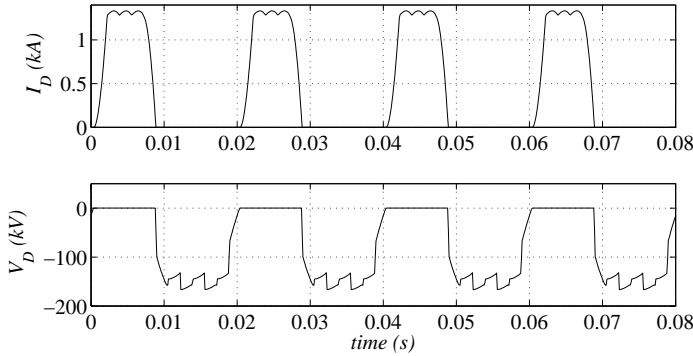| Model	V_{RRM}	$I_{F(AV)M}$	V_{T0}	r_T	
5SDD 10F6000	6 kV	1 363 kA	1.015 V	0.407 mΩ	nom
			1.015 V	0.350 mΩ	25 °C
			0.8 V	0.525 mΩ	150 °C
5SDD 31H6000	6 kV	3 246 kA	0.894 V	0.166 mΩ	nom
			1.0 V	0.105 mΩ	25 °C
			0.8 V	0.188 mΩ	150 °C

Fig. 7.   Current and voltage waveforms through a diode valve at full load

period [16], [17], [20]:

$$P_{conD} = 12N\frac{\omega}{2\pi} \int_{t_s}^{t_s+\frac{2\pi}{\omega}} i_D\left(\tau\right) v_D\left(i_D\left(\tau\right)\right) d\tau \qquad (8)$$

where $N = 30$ is the number of devices per single valve [21], i_D is the diode current and v_D is the diode forward voltage, which is approximated as:

$$v_D(i_D) = V_{T0} + r_T i_D \qquad (9)$$

where V_{T0} is the diode threshold voltage and r_T the diode dynamic resistance. This simple model fits well the actual characteristics of the considered devices.

The current and voltage through a diode valve are shown in Fig. 7. These waveforms are then used to determine the overall
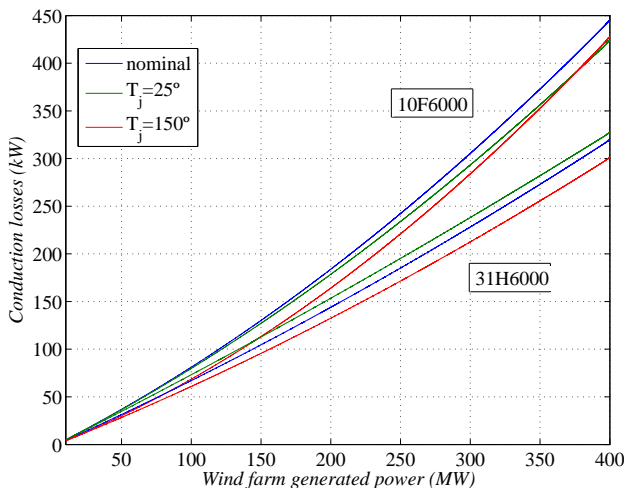

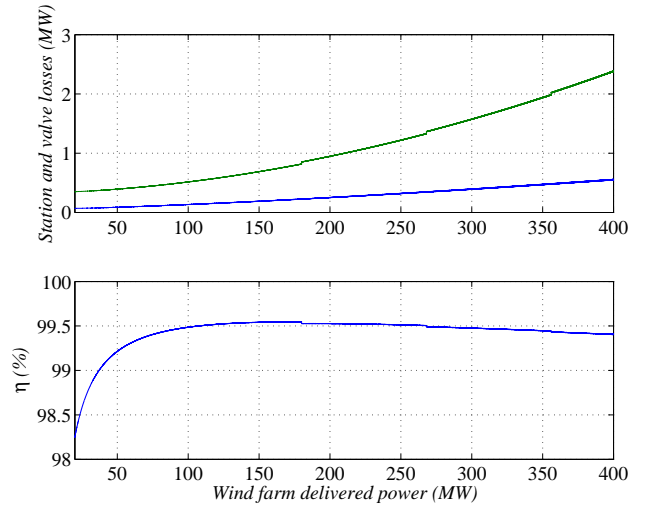Fig. 8.   Diode based HVDC rectifier conduction losses

Fig. 9.   Station losses, valve losses and station efficiency

conduction losses shown in Fig. 8. It is worth stressing that worst case, rated load conduction losses represent only 0.11% of the total delivered power.

Note the loss variation with the temperature and, more importantly, with the selected device. In some cases, it might be advantageous to choose a higher rated device if the additional expense is offset by savings on conduction losses, damping circuits and transformer.

To obtain total valve losses, grading resistors, damping circuits and turn off losses are calculated, as per [16].

The following data is considered for the loss calculation: grading resistors of 0.5M Ω in parallel with each device, RC snubber with $R = 47\ \Omega$ and $C = 0.2\ \mu$F per device, and $Q_{rr} = 3000\ \mu$C, with a maximum $\frac{di_D}{dt} = -1.2A/\mu$s, and overlap angles ($\mu$) directly obtained from the simulation.

Note the resistor and capacitor values for the snubber are typical values and should be tailored to the specific installation. Spread loss for the diode rectifier is not considered.

B. Total station losses

Losses on transformers, smoothing reactor, ac filters and ancillary equipment are estimated from actual data in [19].

It has been assumed that load transformer and smoothing reactor load losses are proportional to the square of the RMS current flowing though them, whereas ancilliary equipment consumption is assumed to increase linearly with load from its no-load value.

A total of four capacitor and filter banks have been considered. Their losses are assumed to be proportional to the number of filter banks connected, which, in turn, are a function of the delivered active power.

Fig. 9 shows an estimate of the valve and rectifier station losses, together with the overall HVDC rectifier station total efficiency, as a percentage of the delivered power.

It is worth noting that total losses when delivering 400 MW are around 0.6%, which is consistant with typical losses of 0.8% for currently installed thyristor based HVDC rectifier stations.

This article has been accepted for publication in a future issue of this journal, but has not been fully edited. Content may change prior to final publication.
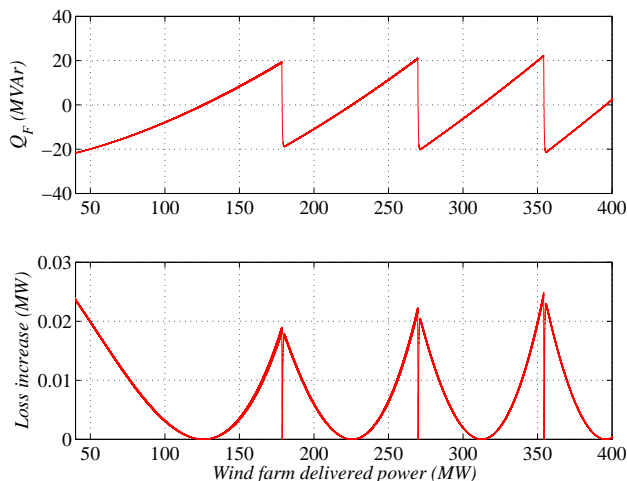
5

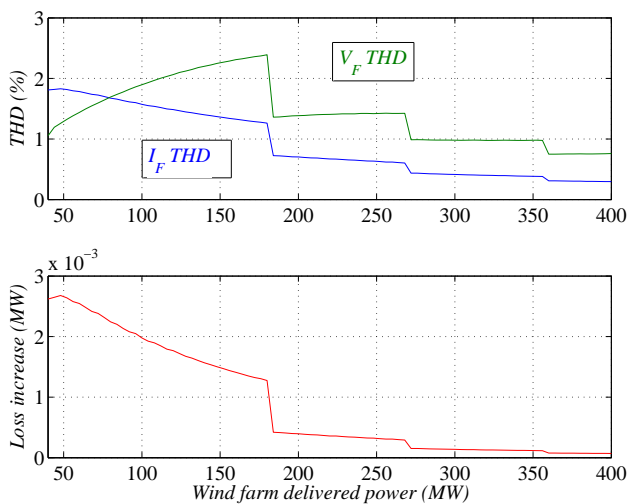Fig. 10.   Wind farm reactive power and corresponding additional losses

Fig. 11.   Wind farm voltage and current THD and corresponding additional conduction losses

C. Harmonic contents and wind turbine loss increase

The use of a diode based HVDC rectifier instead of a VSC-HVDC rectifier station implies that the wind farm should provide additional reactive power and bear additional harmonic currents.

Fig. 10 shows the reactive power to be supplied by the wind farm as a function of the delivered power. The four capacitor and filter banks are switched on and off depending on the delivered power.

The reactive power to be supplied by the wind farm creates additional conduction losses in the wind turbine front-end converter, transformer and in the lines. Assuming overall 2% losses for these components, the additional losses due to the reactive power requirements are shown in Fig. 10.

Fig. 11 shows the total harmonic distortion (THD) on the total wind farm current (I_F) and voltage (V_F), as well as the additional conduction losses caused by the increased harmonic content.

The effects of both the increased reactive power requirements and increased harmonic contents is very small when

compared to total rectifier station losses. In fact, the additional conduction losses due to the harmonic distortion can be safely neglected. Additional hysteresis and eddy-current losses in the wind turbine transformer are even smaller.

D. Comparison with a VSC-HVDC rectifier station

A detailed study on the losses of Modular Multilevel Converters shows that device conduction and switching losses can be as low as 0.7% when the converter is operating as a rectifier ($\cos \phi = -1$) [20]. The study is based on a medium voltage converter, but these figures could be extrapolated to higher voltage converters.

However, the study in [20] did not take into account capacitor, grading losses, filters, inductors, transformer and ancillary equipment.

If these additional components are taken into account, VSC-HVDC station losses up to 1.6% are not uncommon [22]. Therefore, the obtained 0.6% overall losses for the diode rectifier option compare favourably with those of a VSC-HVDC station.

A more thorough comparison of both solutions in terms of losses should require the knowledge of the wind regime at the particular wind farm location, as losses are strongly dependent on delivered power.

V. Fault Ride-through Performance

This section includes the response of the system to faults at the on-shore PCC, wind farm and HVDC line. For all the transients it is assumed that there is enough wind resource and that the wind turbine dynamics are much slower than the electric dynamics, so full power is available after the fault has been cleared.

A. Response to On-shore PCC Short-Circuits

Figs. 12 and 13 show the system behavior during a solid short-circuit at the on-shore PCC while the system is operated at rated power.

When the short-circuit occurs ($t = 0.1$ s), the voltage at the PCC is zero, therefore, it is not possible to deliver active power to the transmission network, i.e. $P_{Vdc} \approx P_S = 0$ pu.

Moreover, the wind turbine front-end converters cannot reduce their generated power instantaneously, therefore $P_{Rdc} \approx P_{Idc} > P_{Vdc}$ from $t = 0.1$ to $t = 0.113$ s. The injected power will lead E_R to increase to 1.15 pu. This behaviour is shown in detail in Fig. 13. To reduce the dc-overvoltage, a braking resistor or a surge arrester is used at the onshore converter station [23].

The increase on E_I at $t = 0.1$ s leads to an increase on the wind farm voltage V_{Fd}. This increase is used for on-shore short-circuit detection by the individual wind turbines. At this point, the wind turbine control system reacts by reducing the off-shore voltage reference V_{Fd}^* from 1.06 to 0.82 pu. Therefore, the off-shore ac-voltage will be smaller than the minimum required for the HVDC diode rectifier to conduct and the off-shore ac-grid will return to islanded operation.

This article has been accepted for publication in a future issue of this journal, but has not been fully edited. Content may change prior to final publication.
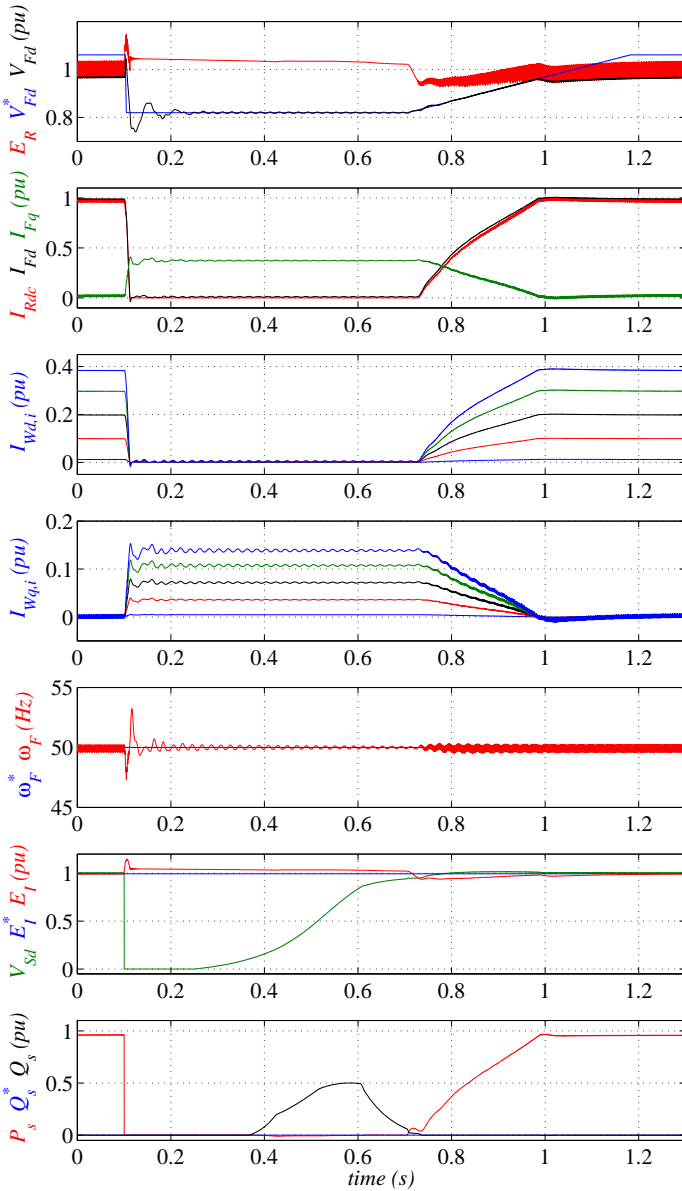
6

Fig. 12. Ride-through performance to on-shore PCC short-circuits

Fig. 14 shows the Voltage Dependant Current Order Limit (VDCOL) used to limit the current delivered by the VSC inverter ($|I_V|_{max}$) during short-circuits.

As a result, the VSC currents I_{Vabc} decrease to 0 pu in about 50 ms with a -3.1 kA overcurrent during 2 ms in phase b of I_V (Fig. 13).

When the fault is cleared and the on-shore PCC voltage V_{Sd} increases and the on-shore VSC can start delivering active power. At this point, the on-shore short-circuit detection system will increase the VSC current limit and command the wind farm to ramp-up the off-shore grid voltage reference V_{Fd}^*.

The off-shore front-end reactive currents (I_{Wqi}) increase during the short-circuit to compensate the reactive power of the rectifier capacitor and filter banks. During the complete transient, the off-shore ac-grid frequency is close to 50 Hz and all voltages and currents are kept under control and within operational ranges of the different elements.
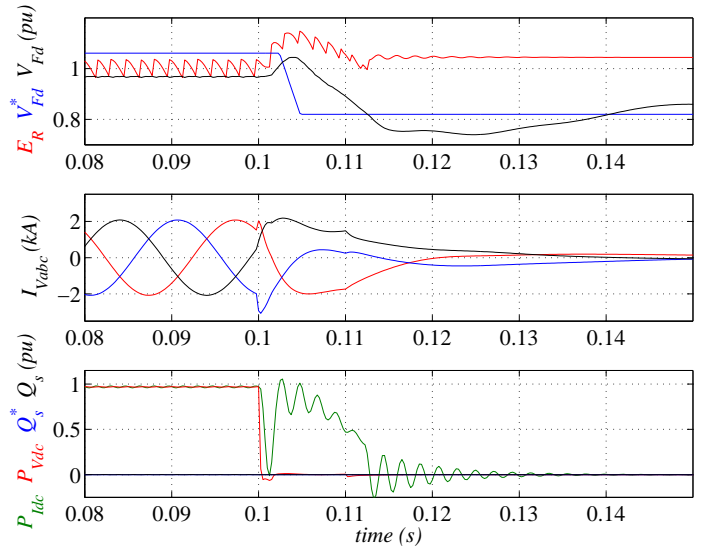
Fig. 13. On-shore PCC short-circuit ride-through (detail)
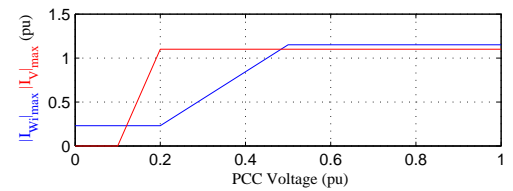
Fig. 14. Front-end-i and VSC inverter maximum current limits

The wind farm remains connected to the grid during the short-circuit. Moreover, Fig. 12 shows reactive power Q_S being supplied by the VSC to support the on-shore grid voltage according to grid code requirements [24].

Fig. 15 shows a good agreement between the reactive current I_r from the Spanish grid code [24] and the reactive current $-I_{Vq}$ from the simulation.

B. Response to Wind Farm ac-grid Faults

Figs. 16 and 17 show the system response to a 400 ms off-shore ac-grid short-circuit when delivering rated power.

During the short-circuit the diode rectifier stops conducting ($I_{Rdc} = 0$ pu), after a delay determined by the rectifier

Fig. 15. Spanish grid code for voltage support during PCC short-circuit

This article has been accepted for publication in a future issue of this journal, but has not been fully edited. Content may change prior to final publication.

7
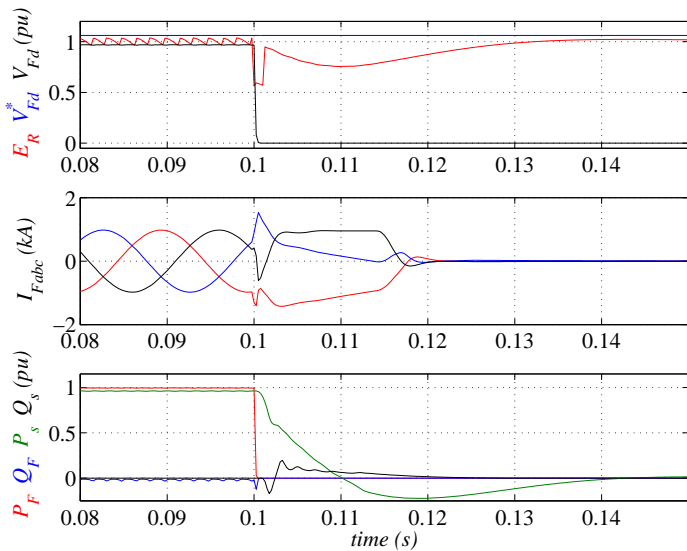
transformer leakage impedance. Therefore, a voltage glitch on E_R appears during the fast reduction of the I_{Rdc} current.

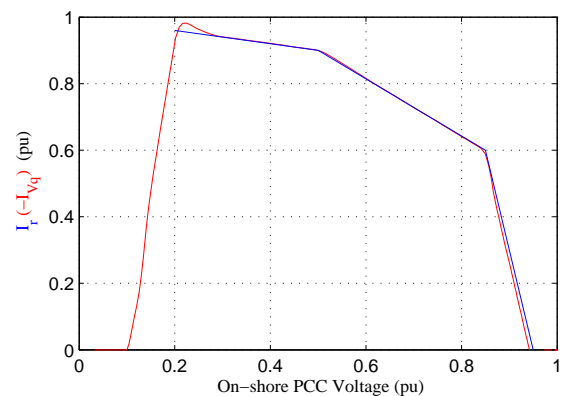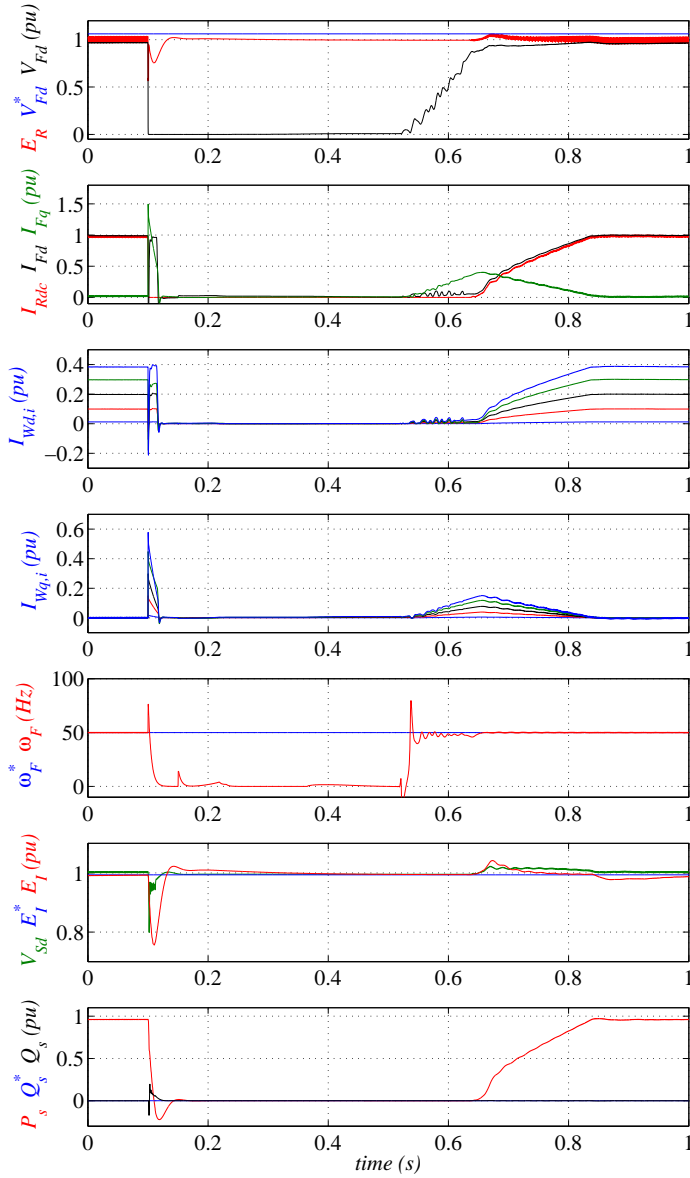Fig. 14 shows the Voltage Dependant Current Order Limit (VDCOL) used to limit the current delivered by the wind turbines ($|I_{Wi}|_{max}$) during short-circuits.

During the short-circuit the off-shore voltage and frequency references do not change.

When the fault is cleared, the V_{Fd} voltage increases and consequently the VDCOL increases the front-end converter current limits. At this stage, wind farm currents and delivered active powers (P_F and P_S) increase smoothly to their pre-fault values.

Fig. 17 shows the detailed HVDC link voltage E_R glitch, together with the wind farm current, and delivered active powers at the onset of the fault. The wind farm currents are reduced to zero in about 20 ms with a peak overcurrent of 1.5 kA.

C. Response to HVDC Link Faults

Most VSC-HVDC converter topologies include free-wheeling diodes. Therefore, during a HVDC line short circuit, the onshore VSC converter cannot, by itself, block the fault current flowing from the transmission line to the HVDC link.

Therefore, ac or dc switchgear needs to be included in order to block fault currents. Ac-grid breakers are usually preferred due to their reduced cost and greater availability.

Fig. 18 shows the behaviour of the proposed system to a mid-point short-circuit on the HVDC line, considering also the coordination with the on-shore ac-grid breaker. When the fault occurs ($t = 0.1$ s), the on-shore ac-breaker detects the I_s overcurrent and trips, so the HVDC inverter station becomes disconnected from the transmission grid.

Simultaneously, the wind turbines detect the short circuit by monitoring local variables, and consequently reduce the off-shore ac-voltage reference V_{Fd}^* to 0.1 pu.

When the HVDC line fault is cleared ($t \approx 0.4$ s), the HVDC voltage E_R increases. As E_R reaches 0.1 pu, the off-shore ac-grid voltage command (V_{Fd}^*) is ramped up.

At this stage the diode rectifier station is conducting. Therefore, the HVDC link voltage increases as V_{Fd} rises to its rated value.

When the on-shore inverter station detects that the HVDC line is energized (i.e. $E_I > 0.95$ pu, $y = 0.55$ s), the station main breaker is closed again. The VSC-HVDC inverter takes over HVDC voltage regulation, thus returning to normal operation. Rated active power delivery is completely restored 0.6 s after the fault.

During the short-circuit, the diode station dc current (I_{Rdc}) reaches a maximum of 2.5 pu, and stays above rated current for about 120 ms. These operating conditions should be taken into account when selecting the devices for the rectifier valves.

It is worth stressing that the proposed protection sequencing allows for direct HVDC line energisation by the wind farm. Therefore, a truly black-start operation of the complete system is performed, even if there is a complete black-out in the on-shore transmission network.
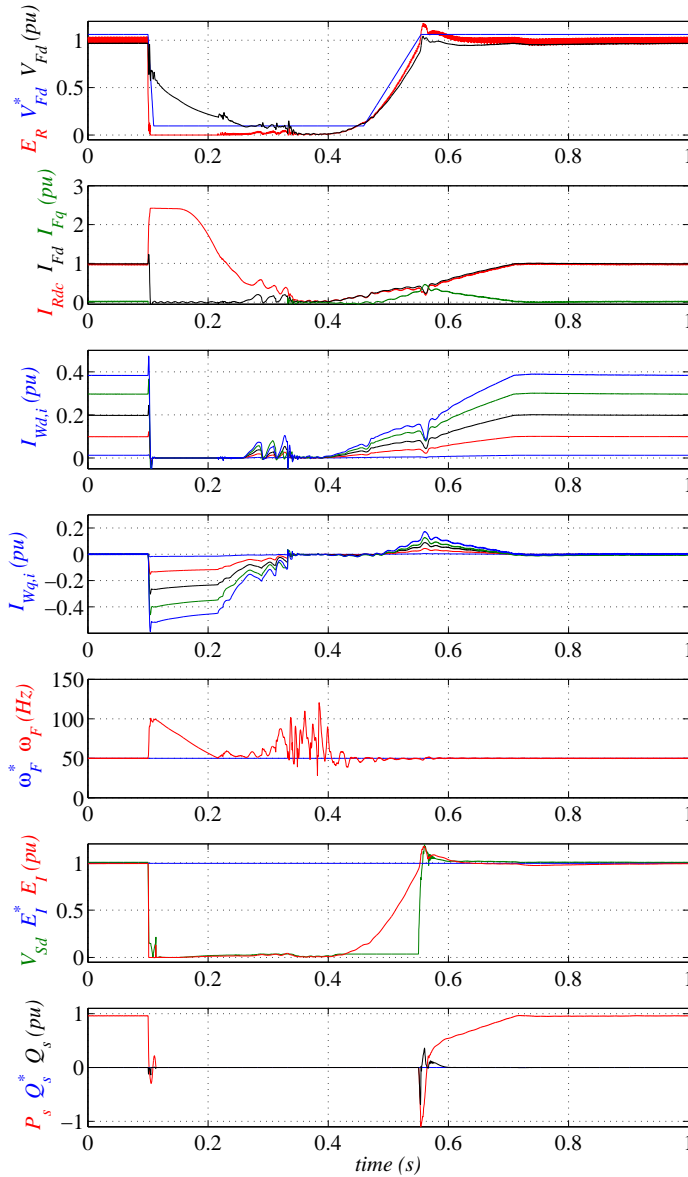

Fig. 16. Wind farm response to off-shore short-circuit

Fig. 17. Wind farm response to off-shore short-circuit (detail)

Fig. 18. Ride-through performance to HVDC link short-circuits

considering faults at the on-shore PCC, at the wind farm off-shore grid and at the midpoint of the HVDC line.

A distributed protection strategy has been devised, so each wind turbine reacts to the different faults using mainly local measurements.

It has been found that, with the additional help of a brake resistor or a surge arrester, the proposed protection mechanism is capable of keeping the HVDC link voltage below 1.15 pu during on-shore inverter PCC short-circuits.

Moreover, during wind farm grid faults, the currents from the wind farms are reduced to zero in less than 20 ms.

During HVDC line short circuits the system is capable of resuming rated power delivery in less than 0.6 s, assuming that the fault is cleared. Additionally, black-start operation of the complete system has been shown, without the help of the on-shore network.

The proposed control system shows good active and reactive power sharing between the wind turbines both during normal operation and during transients.

Therefore, it has been shown that the use of the proposed diode rectifier VSC-HVDC inverter link is technically viable and shows relative advantages in terms of efficiency and fault ride-through performance.

APPENDIX

Aggregated Wind Turbines		
Front-end: 5.4 kVcc, 2 kVac, 50 Hz		
T_{Wi}: 2/345 kV	$R_{Wi} = 0.005$ pu	$L_{Wi} = 0.06$ pu
Rated powers: 5,40,80,120,155 MVA		
HVDC Rectifier (based on Cigre benchmark model [25])		
Capacitor Bank: $C_F = 1.047~\mu$F		
ZF-low frequency filter		
$C_{a1} = 2.094~\mu$F	$C_{a2} = 23.27~\mu$F	$L_a = 435.4$ mH
$R_{a1} = 94.99~\Omega$	$R_{a2} = 835.8~\Omega$	
ZF-high frequency filter		
$C_b = 2.094~\mu$F	$R_b = 265.9~\Omega$	$L_b = 43.41$ mH
Transformer T_R		
345/128 kV, 242 MVA	$L_{R,lk} = 0.18$ pu	$L_{R,m} = 0.01$ pu
dc-smoothing reactor: $L_R = 0.1$ H		
HVDC Cable T-model (100 km) [26]		
$C_H = 40~\mu$F	2 x L_H =2 x 6 mH	2 x R_H =2 x 1.7 Ω
HVDC VSC and ac-grid		
VSC: 300 kVcc, 400 MW, 150 kVac, 50 Hz, $C_I = 35.5~\mu$F		
T_V: 150/400 kV, 500 MVA, $R_V = 0.01$ pu, $L_V = 0.07$ pu		
ac-grid: 400 kV, 500 MVA, Scc=2.5 pu		
VSC PI Controller Parameters		
d-current:	$K_P = 3.1122$	$K_I = 342$
q-current:	$K_P = 3.1122$	$K_I = 342$
dc-voltage:	$K_P = 694.5 \times 10^{-6}$	$K_I = 4.63 \times 10^{-3}$

VI. DISCUSSION AND CONCLUSIONS

This paper has presented a technical feasibility study on the use of a hybrid diode rectifier-VSC inverter HVDC link for the connection of large off-shore wind farms.

The validation of the complete system has been carried out by means of detailed PSCAD simulations, considering a 2.5 SCR at the on-shore PCC. Both islanded operation and optimum power tracking for realistic wind conditions have been verified.

A loss analysis has been carried out, and has been found that the total losses of the diode rectifier station, including the loss increase on wind turbine transformers and front-end converters rise to 0.61% at rated power. This figure compares favourably with the 0.7% device losses reported in [20] for modular multi-level converters and total VSC station losses of 1.6% reported in [22].

A detailed fault ride-through study has been carried out,

REFERENCES

[1] T. Machida, I. Ishikawa, E. Okada, and E. Karasawa, "Control and protection of HVDC systems with diode valve converter," *Name: Electr. Eng. Jpn.(Engl. Transl*, 1978.
[2] J. Bowles, "Multiterminal HVDC transmission systems incorporating diode rectifier stations," *Power Apparatus and Systems, IEEE Transactions on*, vol. PAS-100, no. 4, pp. 1674–1678, 1981.

This article has been accepted for publication in a future issue of this journal, but has not been fully edited. Content may change prior to final publication.

9

[3] S. Hungsasutra and R. Mathur, "Unit connected generator with diode valve rectifier scheme," *IEEE Transactions on Power Systems*, vol. 4, no. 2, pp. 538–543, May 1989.

[4] R. Blasco-Gimenez, S. Añó-Villalba, J. Rodriguez-D'Derlée, S. Bernal-Pérez, and F. Morant, "Diode-Based HVdc link for the connection of large offshore wind farms," *Energy Conversion, IEEE Transactions on*, vol. PP, no. 99, pp. 1–12, 2011.

[5] R. Blasco-Gimenez, S. Añó-Villalba, J. Rodríguez-D'Derlée, F. Morant, and S. Bernal-Pérez, "Distributed voltage and frequency control of offshore wind farms connected with a Diode-Based HVdc link," *Power Electronics, IEEE Transactions on*, vol. 25, no. 12, pp. 3095–3105, 2010.

[6] L. Weimers, "HVDC light: A new technology for a better environment," *Power Engineering Review, IEEE*, vol. 18, no. 8, pp. 19–20, 1998.

[7] G. Asplund, "Application of HVDC light to power system enhancement," in *Power Engineering Society Winter Meeting, 2000. IEEE*, vol. 4, 2000, pp. 2498–2503 vol.4.

[8] S. Nishikata and F. Tatsuta, "A new interconnecting method for wind Turbine/Generators in a wind farm and basic performances of the integrated system," *IEEE Transactions on Industrial Electronics*, vol. 57, no. 2, pp. 468–475, Feb. 2010.

[9] A. Garcés and M. Molinas, "A study of efficiency in a reduced matrix converter for offshore wind farms," *IEEE Transactions on Industrial Electronics*, vol. 59, no. 1, pp. 184–193, Jan. 2012.

[10] S. Bernal-Pérez, S. Añó-Villalba, R. Blasco-Gimenez, and J. Rodriguez-D'Derlée, "Off-shore wind farm grid connection using a novel diode-rectifier and VSC-inverter based HVDC transmission link," in *IECON 2011 - 37th Annual Conference on IEEE Industrial Electronics Society*. IEEE, Nov. 2011, pp. 3186–3191.

[11] L. P. Lazaridis, "Economic comparison of HVAC and HVDC solutions for large offshore wind farms under special consideration of reliability," Master, Royal Institute of Technology Stockholm, 2005.

[12] N. B. Negra, J. Todorovic, and T. Ackermann, "Loss evaluation of HVAC and HVDC transmission solutions for large offshore wind farms," *Electric power systems research*, vol. 76, no. 11, pp. 916–927, 2006.

[13] M. Eichler, P. Maibach, and A. Faulstich, "Full size voltage converters for 5MW offshore wind power generators," in *Proc. EWEC*, Brussels, 2008, pp. 1–10.

[14] M. Liserre, R. Cárdenas, M. Molinas, and J. Rodriguez, "Overview of Multi-MW wind turbines and wind parks," *IEEE Transactions on Industrial Electronics*, vol. 58, no. 4, pp. 1081–1095, Apr. 2011.

[15] S. Zhang, K. Tseng, D. M. Vilathgamuwa, T. D. Nguyen, and X. Wang, "Design of a robust grid interface system for PMSG-Based wind turbine generators," *IEEE Transactions on Industrial Electronics*, vol. 58, no. 1, pp. 316–328, Jan. 2011.

[16] "IEEE recommended practice for determination of power losses in High-Voltage Direct-Current (HVDC) converter stations," *IEEE Std 1158-1991*, p. 1, 1992.

[17] "IEC 61803 - determination of power losses in high-voltage direct current (HVDC) converter stations with line-commutated converters," 2011.

[18] "IEC 62751-1 (draft) - determination of power losses in voltage sourced converters (VSC) for HVDC systems - part 1: General requirements," 2011.

[19] A Gavrilovic, "High voltage direct current," in *Electrical Engineer's Reference Book*, 14th ed., M.A. Laughton and M.G. Say, Eds. Butterworth-Heinemann, 1985.

[20] S. Rohner, S. Bernet, M. Hiller, and R. Sommer, "Modulation, losses, and semiconductor requirements of modular multilevel converters," *Industrial Electronics, IEEE Transactions on*, vol. 57, no. 8, pp. 2633–2642, Aug. 2010.

[21] H. Huang, M. Uder, R. Barthelmess, and J. Dorn, "Application of high power thyristors in HVDC and FACTS systems," in *17th Conference of Electric Power Supply Industry (CEPSI)*, 2008.

[22] H. Pang, G. Tang, and Z. He, "Evaluation of losses in VSC-HVDC transmission system," in *Power and Energy Society General Meeting - Conversion and Delivery of Electrical Energy in the 21st Century, 2008 IEEE*, Jul. 2008, pp. 1 –6.

[23] F. Schettler, H. Huang, and N. Christl, "HVDC transmission systems using voltage sourced converters designand applications," *Power Engineering Society Summer Meeting, 2000. IEEE*, vol. 2, 2000.

[24] R. E. de España, "Spanish grid code draft P.0.12.2," November 2009. [Online]. Available: http://itn4.ree.es/operacion/pdf/Doc_Trabajo_Req_Tec_Eolicos_y_Fotovoltaicos_web_propuesta.pdf

[25] M. Szechtman, T. Wess, and C. V. Thio, "First benchmark model for HVDC control studies," *Electra*, vol. 135, no. 4, pp. 54–67, 1991.

[26] ABB, *Technical description of HVDC Light Technology*, Elanders, Vasteras POW-0038 rev. 5 2008-03 ed.

Soledad Bernal-Perez received her M.Sc. degree in electrical engineering from Universitat Politecnica de Valencia, Spain, in 1999. From 2001 to 2012 she worked as Radio Engineer, carrying out surveys of Global Maritime Distress Safety Systems (GMDSS) radio installations on board of commercial ships for the main Classification Societies. Since 2003, she has been a lecturer at the Dept. of Electrical Engineering of the Univ. Politècnica de València, where she is currently working towards her Ph.D. degree. Her area of interest is grid integration of off-shore wind farms using HVDC links.

Salvador Añó Villalba received his M.Sc. and Ph.D. degrees in Electrical Engineering from the Universitat Politecnica de Valencia, in 1988 and 1996, respectively. From 1987 to 1989 he worked for the R&D Department of Electronic Traffic S.A. to develop hardware and software for street lighting measuring and automation. In 1988 he joined the Dept. of Electrical Engineering of the Universitat Politecnica de Valencia, where he is currently an Associate Professor. His current research interests include wind energy and electrical machines.

Ramon Blasco-Gimenez (S–'94, M–'96, SM–'10) obtained his BEng degree in Electrical Engineering from the Univ. Politecnica de Valencia (Spain) in 1992 and his PhD degree in Electrical and Electronic Engineering from the University of Nottingham (UK) in 1996. From 1992 to 1995 he was a Research Assistant at the Dept. of Electrical and Electronic Engineering of the University of Nottingham. In 1996 he joined the Dept. of Systems Engineering and Control of the Univ. Politècnica de València, where he is currently an Associate Professor. His research interests include Control of Motor Drives, Wind Power Generation and Grid Integration of Renewable Energy Systems. Dr Blasco-Gimenez has been a co-recipient of the 2005 IEEE Transactions on Industrial Electronics Best Paper Award. Dr Blasco-Gimenez is a registered professional engineer in Spain, a Chartered Engineer in the U.K. and a member of the Institute of Engineering and Technology.

J. Rodríguez-D'Derlée (S–'10) received his B.S. degree in Electronic Engineering from University of Táchira, Venezuela, in 2000 and his M.Sc. degree in Math and Computer Science from University of Carabobo, Venezuela in 2004. He is currently working towards his Ph.D. degree at the Institute of Control Systems and Industrial Computing, Universitat Politecnica de Valencia, Spain, focusing on advanced control systems for offshore wind farm and HVDC Transmission. His research interests include advanced control techniques for renewable energy.